PNAS

Supporting Information for

Critical slowing down of the Amazon forest after increased drought occurrence

Johanna Van Passel, Paulo N. Bernardino, Stef Lhermitte, Bianca F. Rius, Marina Hirota, Timo Conradi, Wanda de Keersmaecker, Koenraad Van Meerbeek, Ben Somers

Johanna Van Passel
Email: johanna.vanpassel@kuleuven.be

This PDF file includes:

Supporting Information Text

Critical slowing down versus critical speeding up. Critical slowing down serves as a well-established indicator of stability loss in dynamic systems (1). This theory assumes that a state variable of a dynamic system, denoted as x, has the capacity to recover from various perturbations back to a previous state. The potential function, U(x), describes its attractors, which are the equilibrium states or stable fixed points towards which the variable gravitates, as well as the boundaries beyond which recovery will not occur. As x approaches a bifurcation point, the potential function loses depth, causing the dominant eigenvalue characterizing the rate of change around the equilibrium to converge to zero. This shallowing of the basin results in larger excursions away from the equilibrium and elongates the recovery process, meaning that the system recovers increasingly slow from small perturbations. Consequently, this phenomenon leads to an increase in the autocorrelation of x (1–3). However, previous research has questioned the effectiveness of critical slowing down as an indicator of systems approaching a stochastically driven critical transition instead of a bifurcation-driven one (4).

Conversely, critical speeding up has emerged as a theoretical alternative for detecting stochastically driven critical transitions (3). This theory assumes a potential function with a fixed depth but a narrowing width following a parameter change. This narrowing induces a rattling effect, facilitating a faster recovery of excursions away from equilibrium, resulting in decreased autocorrelation. Nevertheless, while these excursions away from the stable point may be smaller, they occur more frequently, which can also indicate an increased probability of a critical transition. The concept of critical speeding up has been applied in ecological contexts (5), but has also faced scrutiny within the scientific community (1).

The potential occurrence of critical slowing down of the Amazon forest vegetation after drought events can be explained through ecological insights into the Amazon's response to such events. Prior field observations have documented a decline in tree growth and an increase in tree mortality following natural and experimental drought events (6–8). Consequently, recurring drought events are expected to result in decreased rates of forest recovery, which can be quantified through increased temporal autocorrelation in the time series describing the state of the ecosystem, here the enhanced vegetation index (EVI). Conversely, the occurrence of critical speeding up of the Amazon forest vegetation due to drought events is less readily translated into ecological concepts. According to Titus & Watson (3), systems that are designed or managed in a way that increases resistance, while also increasing their precariousness, can experience unwanted stochastic transitions, thereby undergoing critical speeding up.

Testing critical speeding up of the Amazon forest vegetation after increased drought occurrence. If we were to consider critical speeding up and critical slowing down as theories that are not mutually exclusive, following Rocha (5), then we cannot assume a linear relationship between the temporal autocorrelation (TAC) trend and stability anymore. According to the theory of tipping points (9), variables that drive tipping of the Amazon vegetation via a bifurcation point should lead to an increase in TAC, indicating critical slowing down. On the other hand, variables that push the Amazon towards a stochastically-driven critical transition should be reflected by critical speeding up, or a decreasing trend in TAC. To challenge this assumption of linearity and incorporate the possibility that low (negative) TAC trend values are signals of critical speeding up and high (positive) TAC trend values are signals of critical slowing down, we conducted a reanalysis of the Spatial Simultaneous Autoregressive Lag (SSALM) models in three variations: (i) considering only the pixels with strictly negative TAC trend values (hereafter referred to as the model 1), (ii)

considering only the pixels with strictly positive TAC trend values (referred to as model 2), and (iii) using the absolute value of the TAC trend of all pixels as the response variable (referred to model 3). The results of these models are included in Table S8.

Neither model 1 nor model 2 reveals any explanatory variables with significantly negative effect sizes (Table S8), indicating the absence of variables that significantly decrease the TAC trend, which would be an indication of critical speeding up. Conversely, both models show that higher average drought intensity significantly increases the TAC trend (pointing towards critical slowing down). Furthermore, model 1 identifies significantly positive effects of average drought duration and the interaction of drought frequency and intensity. These findings suggest that droughts in the Amazon forest indeed induce critical slowing down of the forest vegetation, rather than critical speeding up.

Additionally, in model 3, nearly all significant effects are negative (Table S8). This implies that these variables tend to drive the TAC trend closer to zero, contradicting both critical slowing down and critical speeding up. However, the negative effects of the drought-related variables are opposite to those observed in both model 1 and 2, where we allowed the possibility that low and high TAC trend values were signals of critical speeding up and critical slowing down, respectively, and to those observed in the primary SSALM model discussed in the manuscript (Table S2). This suggests that, by removing the assumption of a linear relationship between the TAC trend and stability in model 3, we mask the existing relationship between the TAC trend and drought occurrences.

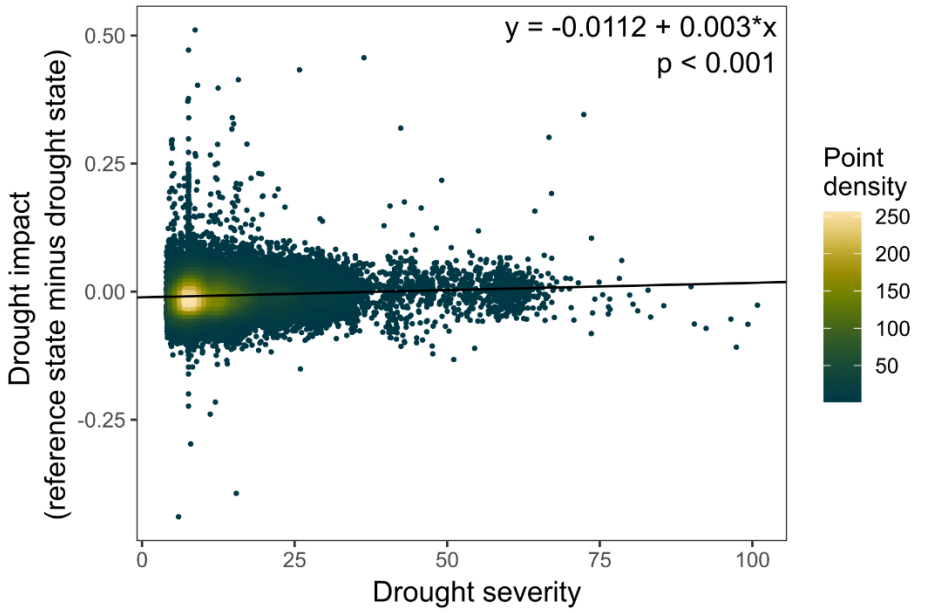

Fig. S1. (Adapted from Figure S5 from Van Passel et al. (10)). Relationship between how much the EVI differed before and during a drought, and the severity of the drought, with a significant positive linear trend. The reference state is fixed per pixel and is the average EVI from January 2001 until December 2002 to limit the effect of previous drought events. The drought state is calculated per pixel as the mean of the EVI values of three months centered around the point in time where the EVI remainder was most negative in the period from the start of the drought until 12 months after the drought had ended. For more details, see ref (10). Positive values on the Y-axis mean that the EVI decreased in the year following the drought. Drought severity (in ref (10) referred to as 'intensity') was computed as the summed integral of all cumulative water deficit anomaly values within a drought period. Consequently, high drought severity can either indicate a prolonged but low-intensity drought, or a shorter but high-intensity drought.

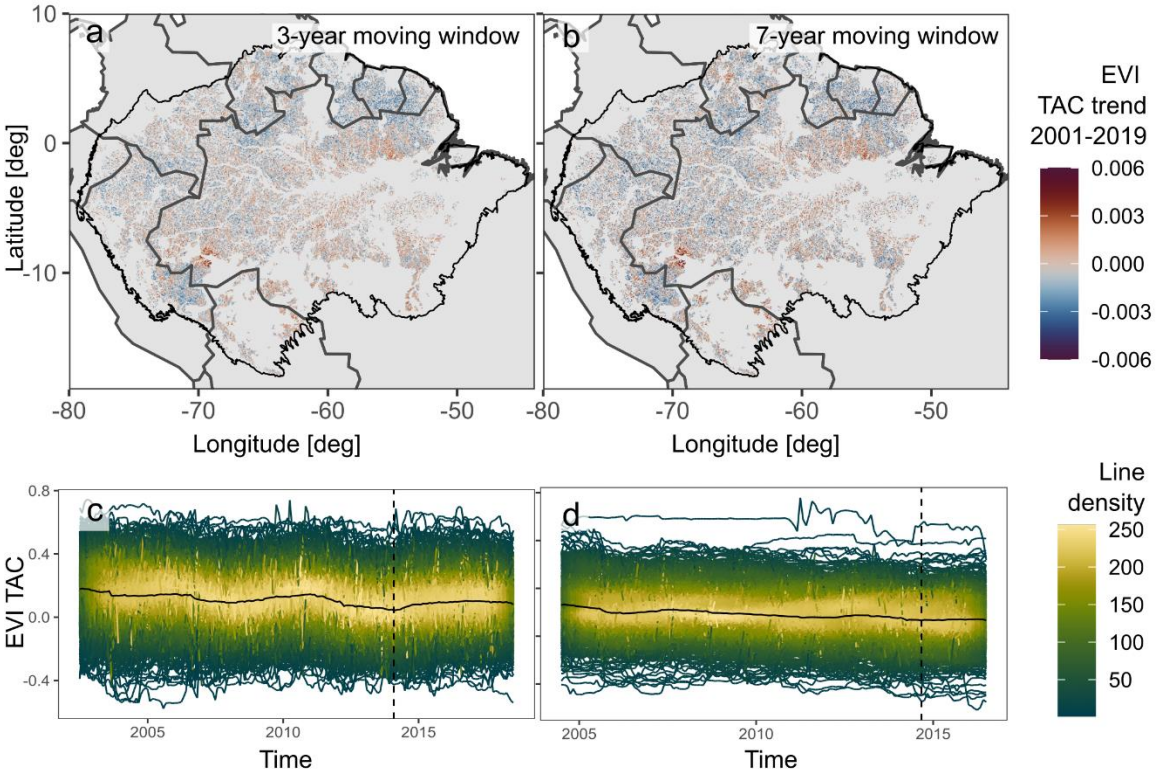

Fig. S2. Comparison of moving window length in temporal autocorrelation (TAC) calculation from EVI time series from 2001 to 2019. (a and c) using a 3-year (36 months) moving window; and (b and d) using a 7-year (84 months) moving window. (a and b) show the trends in TAC across the Amazon forest, while (c and d) show the mean TAC time series across all Amazon forest pixels, plotted in the middle of the moving window, with the density of the TAC time series of 1000 random pixels shown from dark green to yellow. In (c), the lowest mean TAC value happens in February 2014, with the trend from July 2002 until February 2014 and the total trend significantly negative, and the trend from February 2014 until July 2018 significantly positive. In (d), the lowest mean TAC value happens in September 2014, with the trend from July 2004 until September 2014 and the total trend significantly negative, and the trend from September 2014 until July 2016 significantly positive.

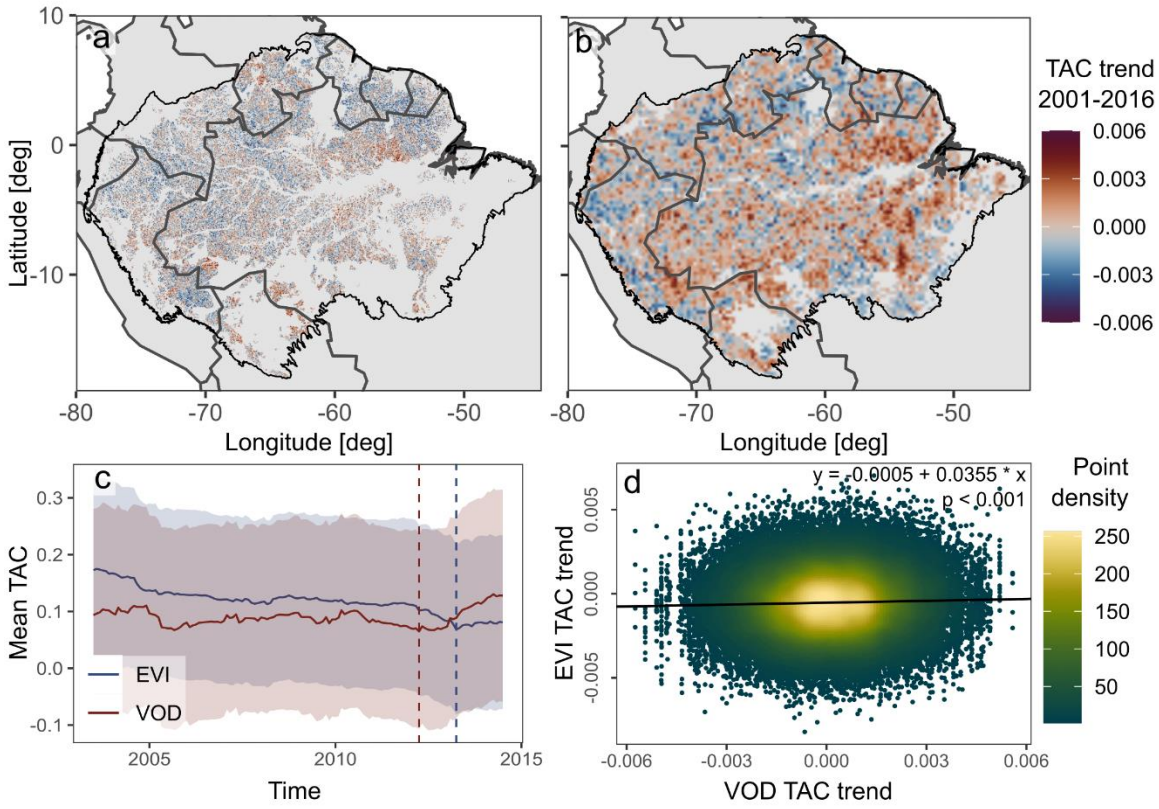

Fig. S3. Comparison of the trend in EVI and VOD TAC for time series from January 2001 until December 2016. (a) EVI TAC trend with a resolution of 0.05°, with 38% of pixels showing an increasing trend in TAC; (b) VOD TAC trend, masked and calculated following Boulton et al. **(11)**, with 50% of pixels showing an increasing trend in TAC; (c) mean TAC across the Amazon forest derived from EVI and VOD time series from July 2003 until July 2014 (values plotted in the middle of the moving window), with the blue and red areas showing ±1 SD. The lowest mean EVI TAC value occurs in April 2013, with the trend up to April 2013 and the total trend significantly negative, and the trend from April 2013 until July 2014 significantly positive. The lowest mean VOD TAC value occurs in April 2012, with the trend up to April 2012 significantly negative, the total trend not significant, and the trend from April 2012 until July 2014 significantly positive. (d) The relation between the downscaled VOD TAC trend and the EVI TAC trend. From dark green to yellow means a higher density of points.

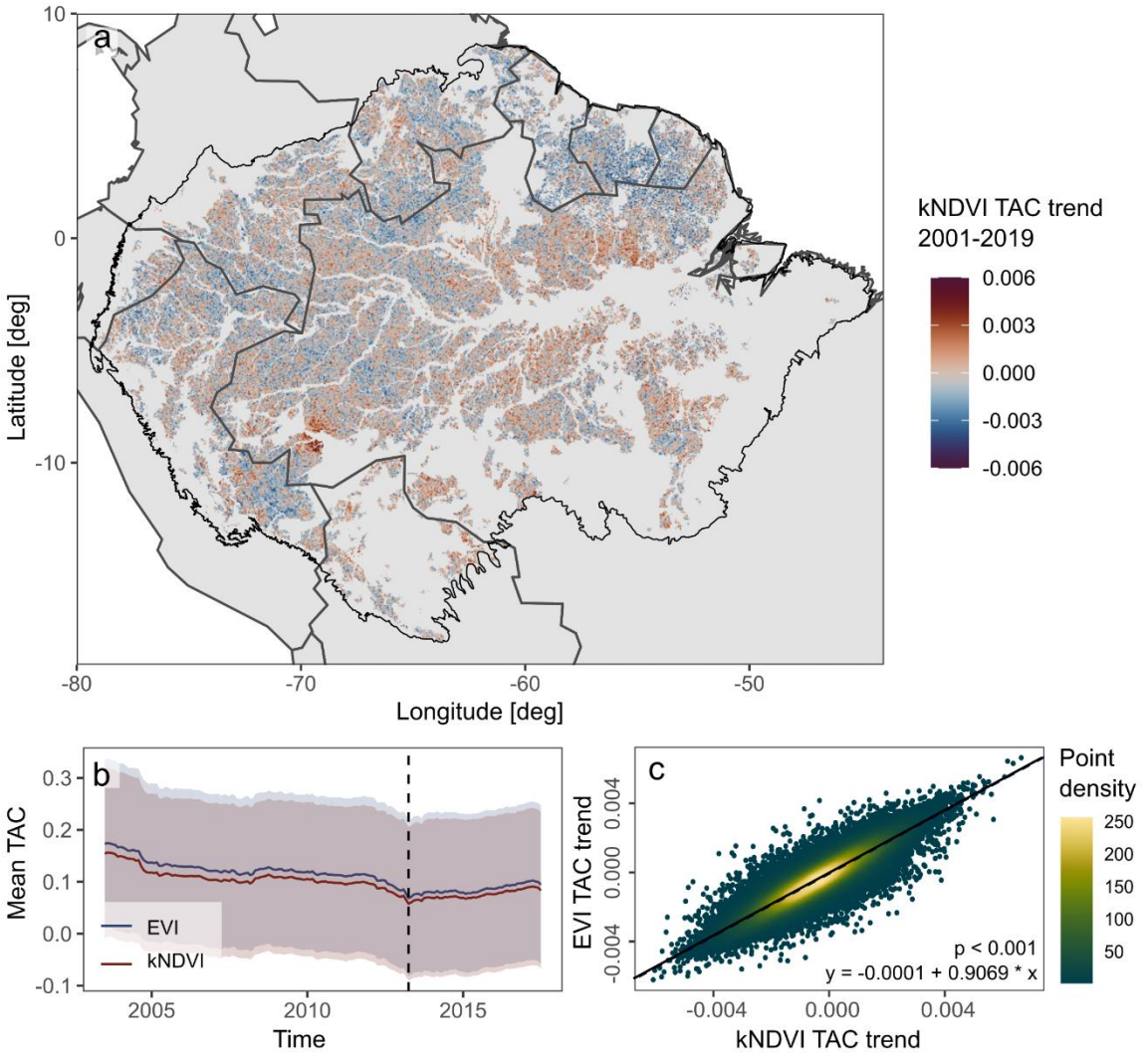

Fig. S4. Comparison of the trend in EVI and kNDVI TAC for time series from January 2001 until December 2019. (a) kNDVI TAC trend, with 39% of pixels showing an increasing trend; (b) mean TAC across the Amazon forest derived from EVI and kNDVI time series, with the red and blue areas showing ±1 SD. The lowest mean EVI and kNDVI TAC values occur in April 2013, with the trends up to April 2013 and the total trends significantly negative, and the trends from April 2013 until July 2017 significantly positive for both vegetation indices. (c) The relation between the TAC trend in EVI and kNDVI. From dark green to yellow means a higher density of points.

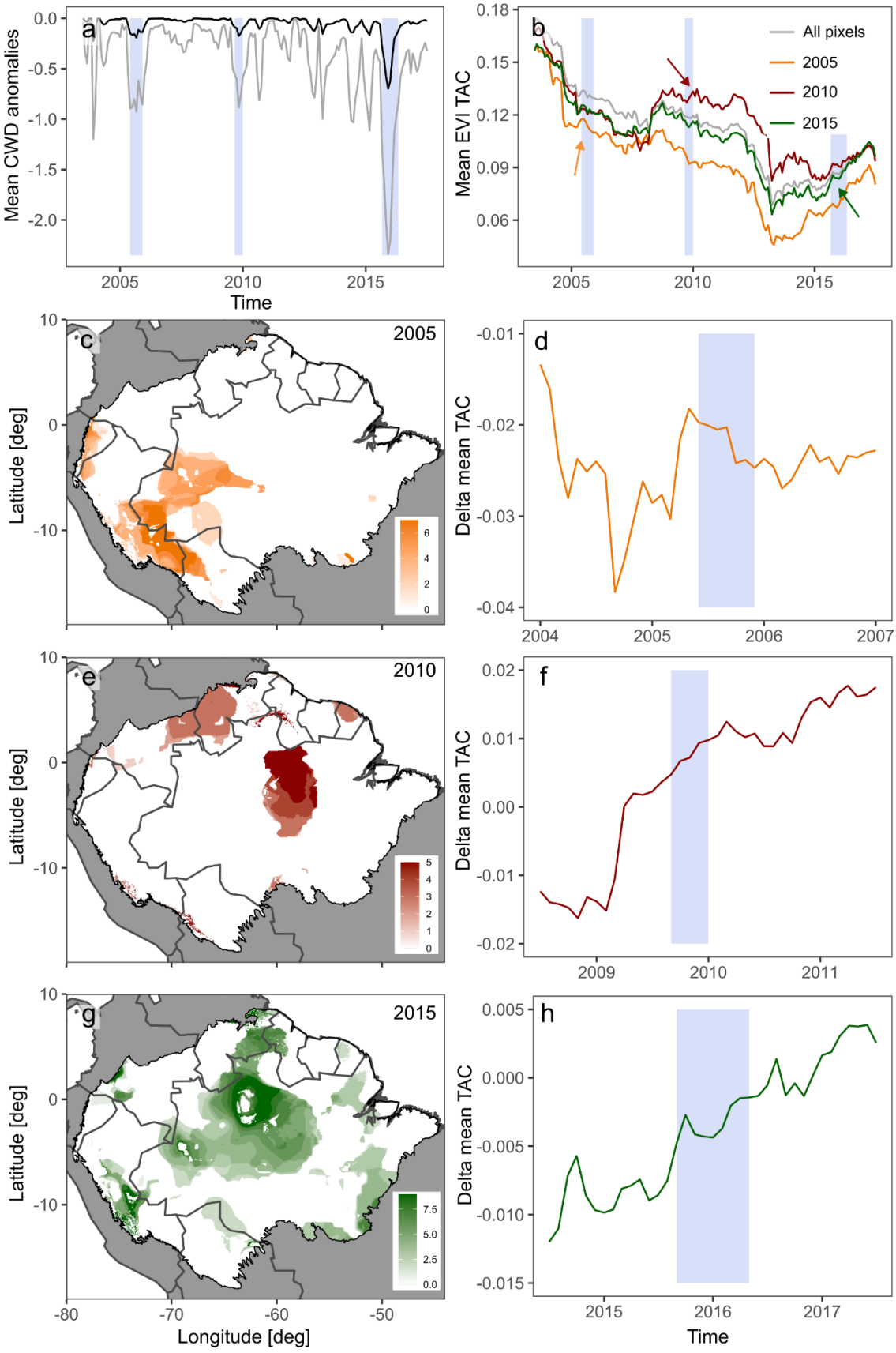
a
Mean CWD anomalies
0.0
-0.5
-1.0
-1.5
-2.0
2005
2010
2015
Time
b
Mean EVI TAC
0.18
0.15
0.12
0.09
0.06
All pixels
2005
2010
2015
c
2005
Latitude [deg]
10
0
-10
6
4
2
0
d
Delta mean TAC
-0.01
-0.02
-0.03
-0.04
2004
2005
2006
2007
e
2010
Latitude [deg]
5
4
3
2
1
0
f
Delta mean TAC
0.02
0.01
0.00
-0.01
-0.02
2009
2010
2011
g
2015
Latitude [deg]
7.5
5.0
2.5
0.0
-80
-70
-60
-50
Longitude [deg]
h
Delta mean TAC
0.005
0.000
-0.005
-0.010
-0.015
2015
2016
2017
Time

Fig. S5. Sensitivity of EVI TAC to widespread drought events. (a) Mean CWD anomalies across the Amazon forest (black line) with widespread drought events (blue boxes) defined as mean values below -0.08 for at least three consecutive months, resulting in three drought events from June to December 2005 ('2005 drought'), September 2009 to January 2010 ('2010 drought'), and September 2015 to May 2016 ('2015 drought'). The grey time series indicates the mean minus the standard deviation of the Amazon-wide CWD anomalies. (b) Mean EVI TAC time series for all pixels that experienced at least one month of drought for each of the three drought periods, with the mean Amazon-wide EVI TAC time series added for comparison. The coloured arrows indicate the visible increase in TAC trend during each of the drought events. (c-e-g) Pixels that experienced the widespread drought events and the number of months that the widespread drought lasted in the (c) 2005, (e) 2010, and (g) 2015 droughts. These included 33,252; 26,534; and 77,517 pixels respectively. (d-f-h) Difference between the mean TAC trend of pixels that did and did not experience the widespread drought event in the (d) 2005, (f) 2010) and (h) 2015 droughts.

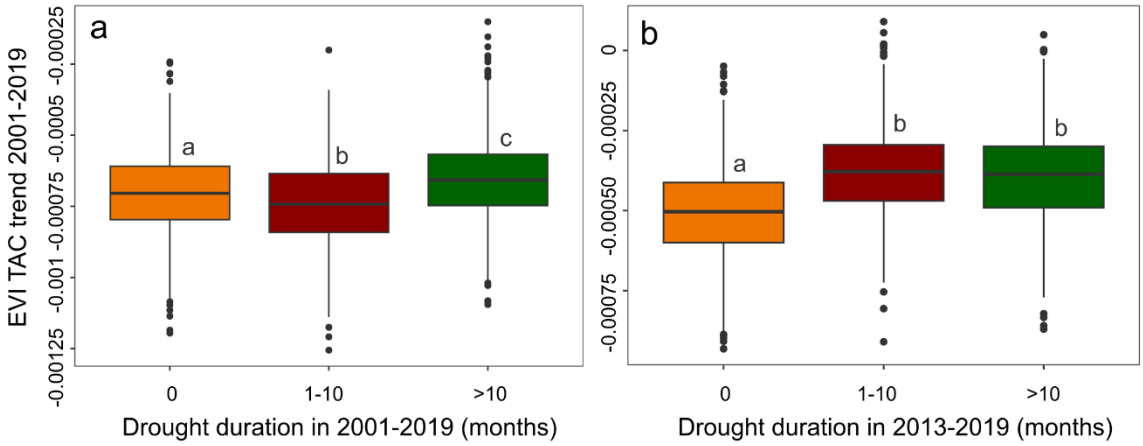

Fig. S6. Sensitivity of EVI TAC trend to different drought history categories. Each category consists of 1,000 times the mean values of 100 randomly chosen pixels to account for the different number of pixels in the three categories. Comparison between total drought duration categories over the time period (a) 2001-2019 and (b) 2013-2019, which is the period in which the mean EVI trend across the whole Amazon is increasing (main Figure 1). In (a) and (b), groups with different letters are significantly different from each other according to the Kruskal-Wallis and post hoc Dunn tests **(12, 13)**.

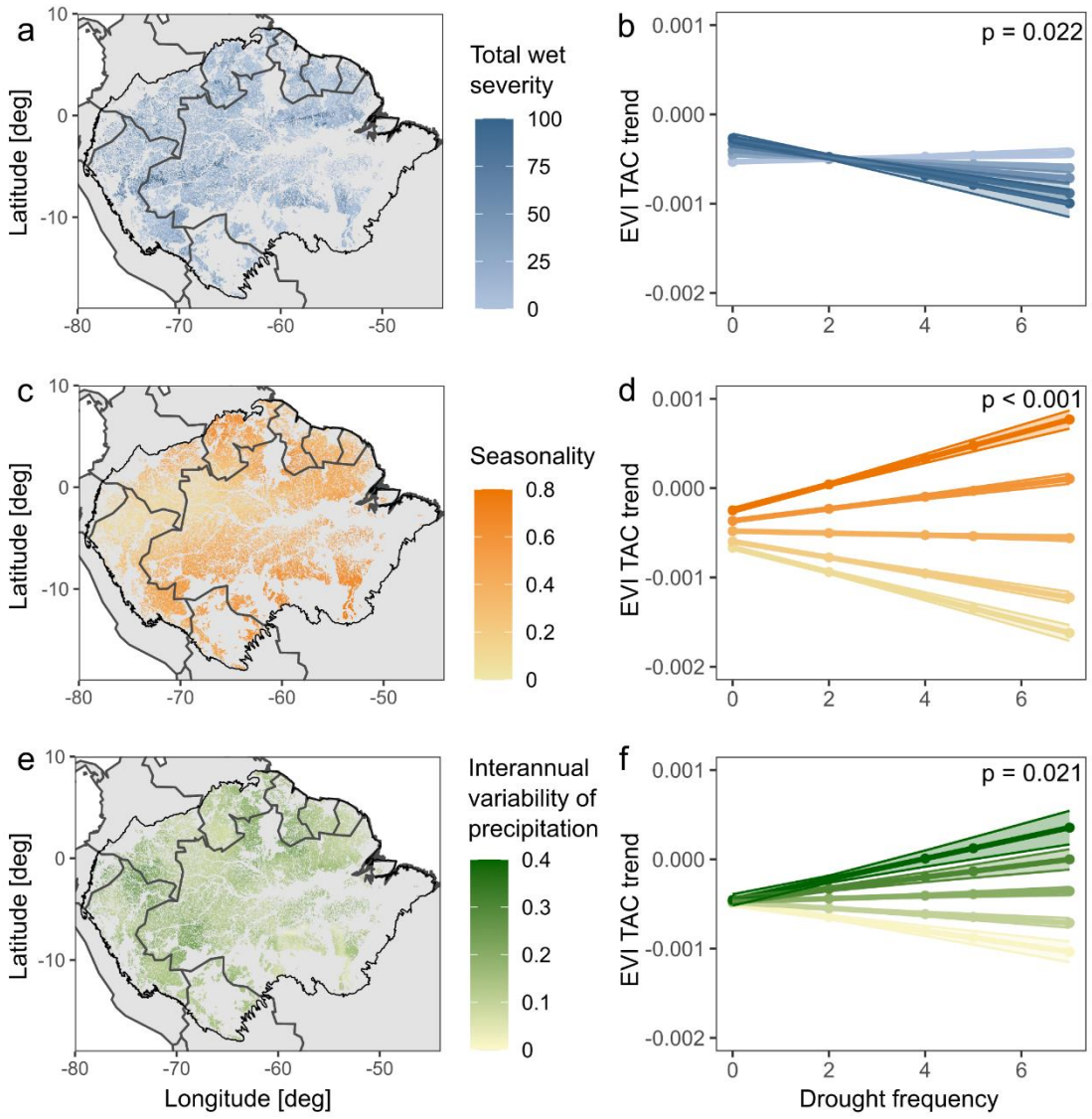

Fig. S7. Environmental drivers of critical slowing down in the Amazon forest and their significant interaction effects in the Amazon-wide model. (a and b) Total severity of wet periods in 2001-2019; (c and d) seasonality; and (e and f) interannual variability of precipitation across the Amazon forest. In (b-d-f), the colored lines indicate how an increase in drought frequency impacts the TAC trend with different levels of total wet period severity, seasonality and interannual variability of precipitation, respectively.

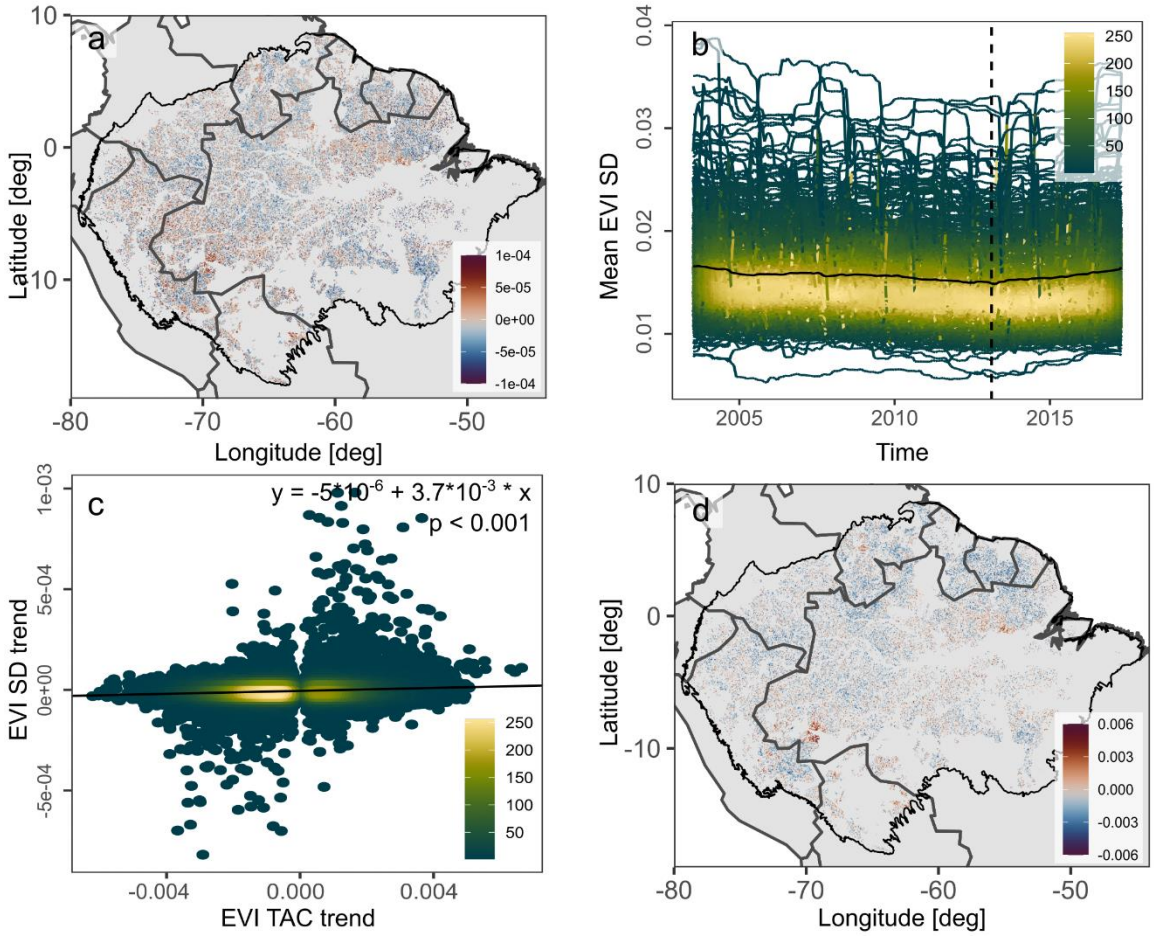

Fig. S8. General trends in EVI standard deviation (SD) across the Amazon forest. (a) EVI SD trend from January 2001 until December 2019, calculated with moving window length of 5 years. (b) Mean EVI SD time series from July 2003 until July 2017 across the Amazon forest (black line) with the density of the SD time series of 1000 random pixels shown from dark green to yellow. In (b), the lowest mean SD value happens in May 2013 (dotted line). (c) Relation between the EVI TAC and SD trends across the Amazon forest. From dark green to yellow means a higher density of points. (d) Significant EVI TAC trends from 2001 until 2019, where the SD trends do not exhibit a significant trend in the other direction.

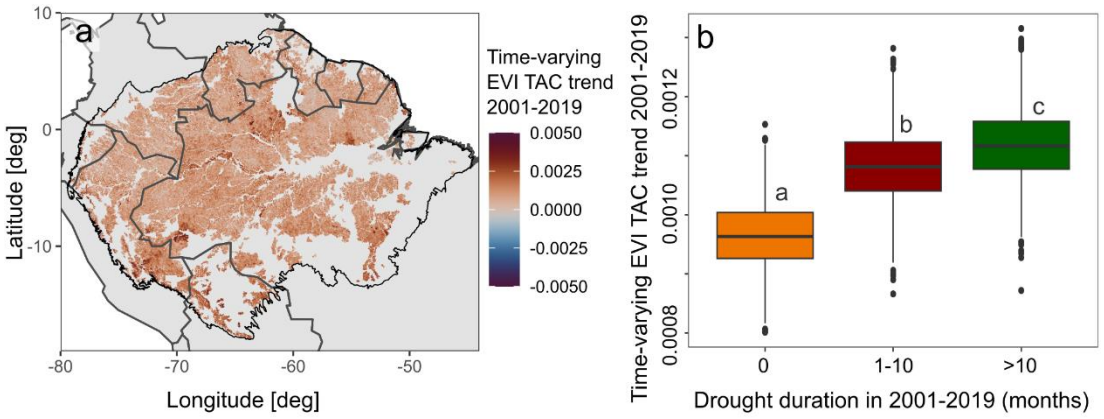

Fig. S9. Time-varying EVI TAC trend and its sensitivity to different drought history categories. (a) Time-varying EVI TAC trend of 2001-2019. 97% of all pixels have an increasing trend. (b) Comparison between total drought duration categories over the time period 2001-2019. Each category consists of 1,000 times the mean values of 100 randomly chosen pixels to account for the different number of pixels in the three categories. In (b), groups with different letters are significantly different from each other according to the Kruskal-Wallis and post hoc Dunn tests **(12, 13)**.

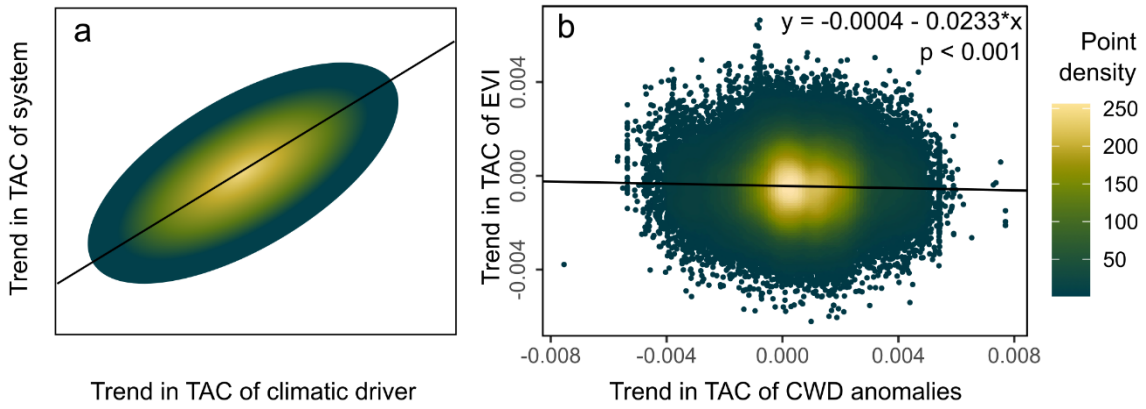

Fig. S10. Testing the presence of confounding effects of changes in TAC of the climate driver that directly affect the system TAC. (a) Expected relation between the trend in TAC of the climatic driver and of the system dynamics, if the temporal dynamics of the TAC of the system are mainly driven by the confounding effects of the changes in autocorrelation of the climate driver; (b) Relation between the trend in TAC of the drought dynamics and the EVI dynamics found in the Amazon. From dark green to yellow means a higher density of points.

Table S1. (continues in next Tables). Coefficient estimates of the Spatial Simultaneous Autoregressive Lag Models (SSALMs) for the 13 woody plant subregional models. Rho is the spatial lag term in the model. Significant variables are indicated with asterisks (*** p < 0.001; ** p < 0.01; * p < 0.05). × = interaction effect with drought frequency.

VARIABLES 2001-2019	REGION 1	REGION 2	REGION 3	REGION 4
Intercept	-4.7×10^{-4} ***	-2.2×10^{-4} ***	-4.4×10^{-4} ***	-6.3×10^{-4} ***
Drought frequency	-2.3×10^{-5}	2.0×10^{-4} ***	7.0×10^{-5}	-5.5×10^{-5}
Average drought intensity	-3.0×10^{-6}	1.4×10^{-4} *	-2.2×10^{-4} *	3.4×10^{-5}
Average drought duration	-8.0×10^{-5}	-8.5×10^{-5}	-2.1×10^{-5}	3.5×10^{-5}
Frequency × average intensity	-2.7×10^{-5}	1.4×10^{-4} **	-8.8×10^{-5}	2.4×10^{-5}
Frequency × average duration	3.4×10^{-5}	1.6×10^{-5}	-5.0×10^{-5}	2.4×10^{-5}
Total severity wet periods	-4.9×10^{-5}	-3.7×10^{-5}	-2.5×10^{-5}	-1.8×10^{-5}
Frequency × severity wet	-1.6×10^{-6}	1.3×10^{-5} **	7.1×10^{-5}	-3.2×10^{-6}
Seasonality	2.0×10^{-4} ***	2.9×10^{-4} ***	1.1×10^{-4} *	1.4×10^{-4} **
Interannual variability of precipitation	1.2×10^{-5}	3.8×10^{-4} ***	-3.1×10^{-5}	7.4×10^{-5}
Frequency × seasonality	-6.5×10^{-5}	-1.8×10^{-5}	-5.9×10^{-5}	1.7×10^{-5}
Frequency × interannual variability	1.0×10^{-4} *	-9.7×10^{-5} *	2.0×10^{-4} **	-5.5×10^{-5}
AIC	-12,383	-12,143	-12,530	-12,609
Rho	0.043	0.164	0.150	0.108
Number of pixels in model	1,200	1,200	1,200	1,200
Nagelkerke R^2	0.03	0.12	0.04	0.03
Bounding box coordinates (xmin, xmax, ymin, ymax)	-79.4°, -62.5°, -12.5°, 3.6°	-79.3°, -61.8°, -18.0°, 1.3°	-74.9°, -58.1°, -9.6°, 4.5°	-73.5°, -59.8°, -8.6°, 7.1°

Table S1. (continued). Coefficient estimates of the Spatial Simultaneous Autoregressive Lag Models (SSALMs) for the 13 woody plant subregional models. Rho is the spatial lag term in the model. Significant variables are indicated with asterisks (*** p < 0.001; ** p < 0.01; * p < 0.05). × = interaction effect with drought frequency.

VARIABLES 2001-2019	REGION 5	REGION 6	REGION 7	REGION 8
Intercept	-3.1×10^{-4} ***	-2.2×10^{-4} ***	-2.8×10^{-4} ***	1.6×10^{-4} ***
Drought frequency	-1.2×10^{-4}	-1.6×10^{-4} **	1.3×10^{-4} *	7.6×10^{-6}
Average drought intensity	-1.5×10^{-4} *	-1.2×10^{-4}	-7.7×10^{-5}	5.1×10^{-5}
Average drought duration	-2.0×10^{-4} *	5.1×10^{-5}	6.6×10^{-5}	3.8×10^{-5}
Frequency × average intensity	-1.6×10^{-5}	-1.6×10^{-4} **	-2.4×10^{-4} ***	4.1×10^{-5}
Frequency × average duration	-2.6×10^{-4} *	2.1×10^{-5}	2.7×10^{-4} **	-4.4×10^{-5}
Total severity wet periods	1.5×10^{-5}	-7.7×10^{-5}	2.2×10^{-5}	6.5×10^{-5}
Frequency × severity wet	1.5×10^{-5}	-7.2×10^{-5}	1.0×10^{-4} *	-9.6×10^{-5}
Seasonality	1.2×10^{-4} *	-4.0×10^{-5}	7.9×10^{-5}	2.0×10^{-4} **
Interannual variability of precipitation	5.4×10^{-5}	4.6×10^{-5}	3.2×10^{-5}	8.1×10^{-6}
Frequency × seasonality	-1.0×10^{-4} *	-5.8×10^{-5}	$4.4 \times 10^{—6}$	-3.2×10^{-5}
Frequency × interannual variability	-4.8×10^{-6}	5.2×10^{-5}	5.9×10^{-5}	1.5×10^{-5}
AIC	-12,563	-12,353	-12,378	-12,599
Rho	0.197	0.111	0.126	0.359
Number of pixels in model	1,200	1,200	1,200	1,200
Nagelkerke R^2	0.05	0.04	0.05	0.13
Bounding box coordinates (xmin, xmax, ymin, ymax)	-73.1°, -58.4°, -7.6°, 8.2°	-68.5°, -55.3°, -8.7°, 2.1°	-68.5°, -52.0°, -15.1°, -5.5°	-69.7°, -57.0°, -19.3°, -8.2°

Table S1. (continued). Coefficient estimates of the Spatial Simultaneous Autoregressive Lag Models (SSALMs) for the 13 woody plant subregional models. Rho is the spatial lag term in the model. Significant variables are indicated with asterisks (*** p < 0.001; ** p < 0.01; * p < 0.05). × = interaction effect with drought frequency.

VARIABLES 2001-2019	REGION 9	REGION 10	REGION 11	REGION 12	REGION 13
Intercept	-1.1×10^{-3} ***	-3.6×10^{-4} ***	-1.0×10^{-3} ***	-2.8×10^{-4} ***	2.7×10^{-4} *
Drought frequency	2.8×10^{-5}	4.7×10^{-5}	-1.5×10^{-5}	-1.1×10^{-5}	2.4×10^{-4}
Average drought intensity	3.3×10^{-5}	-2.4×10^{-4} **	-3.4×10^{-5}	1.8×10^{-4} *	4.3×10^{-4} **
Average drought duration	-6.8×10^{-5}	-7.7×10^{-6}	1.8×10^{-4} **	8.1×10^{-7}	8.7×10^{-5}
Frequency × average intensity	1.2×10^{-5}	4.6×10^{-5}	3.1×10^{-5}	2.8×10^{-4} *	6.2×10^{-4} **
Frequency × average duration	-4.7×10^{-5}	-1.4×10^{-4}	1.3×10^{-5}	-2.1×10^{-4}	2.7×10^{-4} *
Total severity wet periods	-3.6×10^{-5}	3.3×10^{-5}	2.0×10^{-4} ***	-1.4×10^{-4} *	7.2×10^{-5}
Frequency × severity wet	-4.8×10^{-5}	5.5×10^{-5}	-9.0×10^{-5} *	1.1×10^{-5}	7.4×10^{-5}
Seasonality	-1.1×10^{-4}	-2.8×10^{-4} ***	2.9×10^{-4} ***	-1.9×10^{-6}	4.5×10^{-5}
Interannual variability of precipitation	1.8×10^{-4} **	5.8×10^{-6}	-3.2×10^{-4} ***	-1.5×10^{-5}	1.1×10^{-4}
Frequency × seasonality	1.1×10^{-4} *	4.4×10^{-5}	-7.6×10^{-5} *	2.7×10^{-5}	1.5×10^{-4}
Frequency × interannual variability	-1.6×10^{-4} ***	8.4×10^{-5}	2.8×10^{-5}	-3.2×10^{-5}	-9.8×10^{-5}
AIC	-12,514	-12,341	-12,235	-12,329	-5,898
Rho	0.068	0.130	0.105	0.107	0.230
Number of pixels in model	1,200	1,200	1,200	1,200	562
Nagelkerke R^2	0.03	0.08	0.10	0.05	0.13
Bounding box coordinates (xmin, xmax, ymin, ymax)	-62.3°, -52.9°, 1.4°, 8.6°	-65.9°, -49.9°, -1.6°, 8.5°	-63.4°, -50.7°, 0.4°, 5.5°	-68.0°, -44.1°, -10.4°, 8.4°	-63.2°, -43.4°, -14.7°, 1.7°

Table S2. Coefficient estimates of the SSALMs for the Amazon-wide model with different time frames of drought and wet periods included. 2001-2019 is the time period of the TAC trend calculation, and shows the results of the main model, while 1996-2019, 1991-2019 and 1986-2019 extend the time frame for the drought and wet period calculation with 5, 10 and 15 years respectively. Rho is the spatial lag term in the model. Significant variables are indicated with asterisks (*** $p < 0.001$; ** $p < 0.01$; * $p < 0.05$). × = interaction effect with number of droughts.

VARIABLES	**2001-2019 (MAIN MODEL)**	**1996-2019**	**1991-2019**	**1986-2019**
Intercept	-3.2×10^{-4} ***	-3.2×10^{-4} ***	-3.2×10^{-4} ***	-3.1×10^{-4} ***
Drought frequency	-6.9×10^{-6}	-4.7×10^{-6}	2.7×10^{-5} ***	1.8×10^{-5} **
Average drought intensity	6.1×10^{-5} ***	9.1×10^{-5} ***	1.0×10^{-4} ***	9.2×10^{-5} ***
Average drought duration	1.8×10^{-5} **	-3.9×10^{-6}	2.5×10^{-5} *	5.3×10^{-6}
Frequency × average intensity	6.0×10^{-5} ***	8.3×10^{-5} ***	6.9×10^{-5} ***	6.5×10^{-5} ***
Frequency × average duration	8.4×10^{-6}	-2.2×10^{-5} *	5.6×10^{-6}	-1.9×10^{-5}
Total severity wet periods	7.7×10^{-6}	-6.9×10^{-7}	5.3×10^{-6}	-3.5×10^{-5} ***
Frequency × severity wet	-1.3×10^{-5} *	-3.2×10^{-5} ***	-1.9×10^{-5} ***	-2.3×10^{-5} ***
Seasonality	1.2×10^{-4} ***	1.3×10^{-4} ***	1.2×10^{-4} ***	1.0×10^{-4} ***
Interannual variability of precipitation	2.2×10^{-5} ***	2.9×10^{-5} ***	9.6×10^{-6}	1.7×10^{-5} **
Frequency × seasonality	4.1×10^{-5} ***	4.1×10^{-5} ***	5.4×10^{-5} ***	3.4×10^{-5} ***
Frequency × interannual variability	1.2×10^{-5} *	2.1×10^{-5} ***	1.4×10^{-5} **	1.7×10^{-5} ***
AIC	-728,200	-728,270	-728,310	-728,310
Rho	0.345	0.343	0.342	0.342
Number of pixels in model	70,336	70,336	70,336	70,336
Nagelkerke R^2	0.09	0.09	0.09	0.09

Table S3. Coefficient estimates of the SSALMs for the different moving window lengths in the TAC calculation. The TAC calculated with a 3 year moving window leads to a time series from July 2002 until July 2018, while a 7 year moving window leads to a time series from July 2004 until July 2016. Rho is the spatial lag term in the model. Significant variables are indicated with asterisks (*** $p < 0.001$; ** $p < 0.01$; * $p < 0.05$). × = interaction effect with number of droughts.

VARIABLES 2001-2019	3 YEAR MOVING WINDOW	7 YEAR MOVING WINDOW
Intercept	-2.9×10^{-4} ***	-3.4×10^{-4} ***
Drought frequency	-9.6×10^{-6}	-2.8×10^{-6}
Average drought intensity	7.4×10^{-5} ***	4.9×10^{-5} ***
Average drought duration	1.1×10^{-5}	1.4×10^{-5} *
Frequency × average intensity	6.5×10^{-5} ***	5.6×10^{-5} ***
Frequency × average duration	1.5×10^{-6}	-4.3×10^{-5}
Total severity wet periods	1.2×10^{-5} **	5.9×10^{-6}
Frequency × severity wet	-1.1×10^{-5} *	-1.2×10^{-5} *
Seasonality	1.1×10^{-4} ***	1.2×10^{-4} ***
Interannual variability of precipitation	8.0×10^{-6}	3.9×10^{-5} ***
Frequency × seasonality	3.8×10^{-5} ***	3.9×10^{-5} ***
Frequency × interannual variability	1.7×10^{-5} ***	1.4×10^{-5} *
AIC	-747,590	-717,350
Rho	0.371	0.325
Number of pixels in model	70,336	70,336
Nagelkerke R^2	0.11	0.08

Table S4. Coefficient estimates of the SSALMs for the pixels with a significant TAC trend where the SD trend does not exhibit a significant trend in the other direction. Rho is the spatial lag term in the model. Significant variables are indicated with asterisks (*** $p < 0.001$; ** $p < 0.01$; * $p < 0.05$). × = interaction effect with number of droughts.

VARIABLES 2001-2019	TAC AND SD TREND NOT IN OPPOSITE DIRECTION
Intercept	-4.2×10^{-4} ***
Drought frequency	-8.7×10^{-6}
Average drought intensity	5.2×10^{-5} ***
Average drought duration	3.8×10^{-6}
Frequency × average intensity	5.8×10^{-5} ***
Frequency × average duration	-1.1×10^{-5}
Total severity wet periods	1.1×10^{-5}
Frequency × severity wet	-1.1×10^{-5} *
Seasonality	1.1×10^{-4} ***
Interannual variability of precipitation	5.8×10^{-5} ***
Frequency × seasonality	3.7×10^{-5} ***
Frequency × interannual variability	1.6×10^{-5} *
AIC	-392,050
Rho	0.437
Number of pixels in model	37,990
Nagelkerke R^2	0.14

Table S5. Coefficient estimates of the SSALMs for the kNDVI TAC trend model. Rho is the spatial lag term in the model. Significant variables are indicated with asterisks (*** p < 0.001; ** p < 0.01; * p < 0.05). × = interaction effect with number of droughts.

VARIABLES 2001-2019	KNDVI TAC TREND
Intercept	-2.5×10^{-4} ***
Drought frequency	-1.3×10^{-5} **
Average drought intensity	2.8×10^{-5} ***
Average drought duration	1.2×10^{-5} *
Frequency × average intensity	2.9×10^{-5} ***
Frequency × average duration	1.4×10^{-5}
Total severity wet periods	8.3×10^{-7}
Frequency × severity wet	-6.5×10^{-6}
Seasonality	8.0×10^{-5} ***
Interannual variability of precipitation	9.4×10^{-6} *
Frequency × seasonality	3.3×10^{-5} ***
Frequency × interannual variability	7.1×10^{-6}
AIC	-1,111,300
Rho	0.425
Number of pixels in model	107,345
Nagelkerke R^2	0.10

Table S6. (continues in next Table). Mean ± standard deviation of all variables included in the regional SSALMs.

VARIABLES	WHOLE AMAZON	REGION 1	REGION 2	REGION 3	REGION 4	REGION 5	REGION 6
Drought frequency 2001-2019	1.6 ± 1.0	1.6 ± 1.0	1.8 ± 1.0	1.0 ± 1.0	2.0 ± 1.2	1.7 ± 0.8	1.9 ± 0.9
Average drought intensity 2001-2019	3.7 ± 1.8	4.5 ± 1.8	4.1 ± 1.1	3.0 ± 2.6	3.6 ± 1.5	5.2 ± 1.2	4.0 ± 1.3
Average drought duration 2001-2019	3.9 ± 3.3	2.9 ± 1.9	5.5 ± 4.1	2.0 ± 2.0	4.5 ± 2.6	5.8 ± 4.8	4.8 ± 2.8
Total severity wet periods 2001-2019	20.0 ± 16.6	29.6 ± 22.6	20.1 ± 14.3	19.3 ± 11.2	18.2 ± 15.2	19.1 ± 13.2	18.9 ± 17.0
Seasonality	0.40 ± 0.15	0.26 ± 0.10	0.46 ± 0.09	0.25 ± 0.12	0.43 ± 0.12	0.28 ± 0.07	0.43 ± 0.08
Interannual variability of precipitation	0.15 ± 0.04	0.18 ± 0.04	0.16 ± 0.03	0.13 ± 0.04	0.14 ± 0.04	0.14 ± 0.02	0.14 ± 0.02
Mean annual precipitation	2,278 ± 517	2,611 ± 448	2,125 ± 542	2,941 ± 359	2,675 ± 398	2,599 ± 254	2,370 ± 186
Bounding box coordinates (xmin, xmax, ymin, ymax)	-79.4°, -45°, -18.0°, 8.7°	-79.4°, -62.5°, -12.5°, 3.6°	-79.3°, -61.8°, -18.0°, 1.3°	-74.9°, -58.1°, -9.6°, 4.5°	-73.5°, -59.8°, -8.6°, 7.1°	-73.1°, -58.4°, -7.6°, 8.2°	-68.5°, -55.3°, -8.7°, 2.1°

Table S6. (continued). Mean ± standard deviation of all variables included in the regional SSALMs.

VARIABLES	REGION 7	REGION 8	REGION 9	REGION 10	REGION 11	REGION 12	REGION 13
Drought frequency 2001-2019	1.5 ± 1.1	1.3 ± 0.8	2.2 ± 0.8	1.4 ± 1.1	1.2 ± 0.6	1.0 ± 0.7	1.6 ± 0.8
Average drought intensity 2001-2019	3.1 ± 1.8	3.5 ± 1.5	3.9 ± 0.9	2.6 ± 1.7	3.6 ± 1.4	2.6 ± 1.6	4.6 ± 1.0
Average drought duration 2001-2019	3.6 ± 2.6	6.9 ± 9.3	5.5 ± 3.8	3.5 ± 2.6	2.4 ± 1.1	2.4 ± 1.8	4.8 ± 2.0
Total severity wet periods 2001-2019	17.5 ± 12.9	9.8 ± 7.7	22.9 ± 17.3	17.3 ± 16.9	13.5 ± 9.7	15.3 ± 12.9	13.2 ± 6.9
Seasonality	0.58 ± 0.07	0.59 ± 0.04	0.40 ± 0.05	0.48 ± 0.08	0.45 ± 0.03	0.57 ± 0.06	0.69 ± 0.10
Interannual variability of precipitation	0.13 ± 0.04	0.16 ± 0.02	0.15 ± 0.02	0.16 ± 0.03	0.11 ± 0.02	0.14 ± 0.03	0.09 ± 0.03
Mean annual precipitation	2,127 ± 255	1,563 ± 214	2,058 ± 232	2,114 ± 223	2,301 ± 273	2,060 ± 227	1,957 ± 267
Bounding box coordinates (xmin, xmax, ymin, ymax)	-68.5°, -55.3°, -8.7°, 2.1°	-69.7°, -57.0°, -19.3°, -8.2°	-62.3°, -52.9°, 1.4°, 8.6°	-65.9°, -49.9°, -1.6°, 8.5°	-63.4°, -50.7°, 0.4°, 5.5°	-68.0°, -44.1°, -10.4°, 8.4°	-63.2°, -43.4°, -14.7°, 1.7°

Table S7. Coefficient estimates of the SSALMs for the main EVI TAC model with the inclusion of extra environmental variables describing elevation and soil texture. Rho is the spatial lag term in the model. Significant variables are indicated with asterisks (*** p < 0.001; ** p < 0.01; * p < 0.05). × = interaction effect with number of droughts.

VARIABLES	VALUES
Intercept	-3.3×10^{-4} ***
Drought frequency	-1.2×10^{-6}
Average drought intensity	5.2×10^{-5} ***
Average drought duration	1.9×10^{-5} **
Frequency × average intensity	6.0×10^{-5} ***
Frequency × average duration	1.0×10^{-5}
Total severity wet periods	2.6×10^{-6}
Frequency × severity wet	-9.7×10^{-6}
Seasonality	1.2×10^{-4} ***
Interannual variability of precipitation	1.3×10^{-5} *
Frequency × seasonality	5.0×10^{-5} ***
Frequency × interannual variability	1.4×10^{-5} **
Elevation	3.4×10^{-6}
Soil clay	-2.0×10^{-5} **
Soil sand	-6.9×10^{-5} ***
Frequency × elevation	-8.6×10^{-6}
Frequency × soil clay	2.4×10^{-6}
Frequency × soil sand	6.3×10^{-6}
AIC	-728,310
Rho	0.341
Nagelkerke R^2	0.09

Table S8. Coefficient estimates of the SSALMs testing the occurrence of critical speeding up versus critical slowing down. Rho is the spatial lag term in the model. Significant variables are indicated with asterisks (*** p < 0.001; ** p < 0.01; * p < 0.05). × = interaction effect with number of droughts.

VARIABLES	PIXELS WITH NEGATIVE TAC TREND VALUES	PIXELS WITH POSITIVE TAC TREND VALUES	ABSOLUTE VALUE OF TAC TREND OF ALL PIXELS
Intercept	-1.2×10^{-3} ***	9.0×10^{-4} ***	1.1×10^{-3} ***
Drought frequency	5.2×10^{-6}	-9.4×10^{-6}	-6.0×10^{-6}
Average drought intensity	5.4×10^{-5} ***	2.4×10^{-5} **	-2.7×10^{-5} ***
Average drought duration	1.5×10^{-5} **	-7.1×10^{-6}	-1.5×10^{-5} ***
Frequency × average intensity	5.5×10^{-5} ***	7.0×10^{-6}	-3.6×10^{-5} ***
Frequency × average duration	-1.4×10^{-6}	1.7×10^{-5}	4.8×10^{-6}
Total severity wet periods	7.8×10^{-6}	2.8×10^{-6}	-5.5×10^{-6}
Frequency × severity wet	-9.0×10^{-6}	-2.7×10^{-6}	6.0×10^{-6}
Seasonality	4.5×10^{-5} ***	7.4×10^{-5} ***	-8.0×10^{-6}
Interannual variability of precipitation	-3.8×10^{-6}	3.7×10^{-5} ***	1.3×10^{-5} ***
Frequency × seasonality	3.4×10^{-5} ***	1.2×10^{-5} *	-1.8×10^{-5} ***
Frequency × interannual variability	2.3×10^{-5} ***	-6.9×10^{-6}	-1.9×10^{-5} ***
AIC	-492,100	-297,670	-787,170
Rho	0.122	0.123	0.104
Number of pixels	44,202	26,134	70,336
Nagelkerke R^2	0.02	0.03	0.01

SI References

1. T. M. Lenton, *et al.*, A resilience sensing system for the biosphere. *Phil. Trans. R. Soc. B* **377**, 20210383 (2022).

2. M. Scheffer, *et al.*, Early-warning signals for critical transitions. *Nature* **461**, 53–59 (2009).

3. M. Titus, J. Watson, Critical speeding up as an early warning signal of stochastic regime shifts. *Theor Ecol* **13**, 449–457 (2020).

4. A. Hastings, D. B. Wysham, Regime shifts in ecological systems can occur with no warning. *Ecology Letters* **13**, 464–472 (2010).

5. J. C. Rocha, Ecosystems are showing symptoms of resilience loss. *Environ. Res. Lett.* **17**, 065013 (2022).

6. T. R. Feldpausch, *et al.*, Amazon forest response to repeated droughts. *Global Biogeochemical Cycles* **30**, 964–982 (2016).

7. D. C. Nepstad, I. M. Tohver, D. Ray, P. Moutinho, G. Cardinot, Mortality of large trees and lianas following experimental drought in an Amazon forest. *Ecology* **88**, 2259–2269 (2007).

8. J. S. Powers, *et al.*, A catastrophic tropical drought kills hydraulically vulnerable tree species. *Global Change Biology* **26**, 3122–3133 (2020).

9. P. Ashwin, S. Wieczorek, R. Vitolo, P. Cox, Tipping points in open systems: bifurcation, noise-induced and rate-dependent examples in the climate system. *Phil. Trans. R. Soc. A.* **370**, 1166–1184 (2012).

10. J. Van Passel, *et al.*, Climatic legacy effects on the drought response of the Amazon rainforest. *Global Change Biology* (2022) https:/doi.org/10.1111/gcb.16336.

11. C. A. Boulton, T. M. Lenton, N. Boers, Pronounced loss of Amazon rainforest resilience since the early 2000s. *Nature Climate Change* **12**, 271–278 (2022).

12. W. H. Kruskal, W. A. Wallis, Use of ranks in one-criterion variance analysis. *Journal of the American statistical Association* **47**, 583–621 (1952).

13. O. J. Dunn, Multiple comparisons using rank sums. *Technometrics* **6**, 241–252 (1964).